Sfermion pair production in polarized and unpolarized $\gamma\gamma$ collisions

S. Berge, M. Klasen, and Y. Umeda
II. Institut für Theoretische Physik, Universität Hamburg, Luruper Chaussee 149, D-22761 Hamburg, Germany
(Received 9 August 2000; published 3 January 2001)

We calculate total and differential cross sections for the production of sfermion pairs in photon-photon collisions, including contributions from resolved photons and arbitrary photon polarization. Sfermion production in photon collisions depends only on the sfermion mass and charge. It is thus independent of the details of the SUSY breaking mechanism, but highly sensitive to the sfermion charge. We compare the total cross sections for bremsstrahlung, beamstrahlung, and laser backscattering photons to those in e^+e^- annihilation. We find that the total cross section at a polarized photon collider is larger than the e^+e^- annihilation cross section up to the kinematic limit of the photon collider.

DOI: 10.1103/PhysRevD.63.035003 PACS number(s): 14.80.Ly, 12.38.Bx, 13.85.Qk, 13.88.+e

I. INTRODUCTION

Among the possible extensions of the standard model (SM), supersymmetric (SUSY) theories have a variety of attractive features: They can solve the Higgs hierarchy puzzle, break electroweak symmetry radiatively at low energies, and explain the unification of gauge couplings at a high energy scale. A necessary condition for these arguments to be valid is that SUSY is realized in the region of the electroweak scale. This makes the search for supersymmetry one of the most important tasks at future high-energy collider experiments.

If SUSY is realized at the electroweak scale, most of the SUSY partners of the SM particles will be discovered at the high center-of-mass energies available at the next generation of hadron colliders, i.e., at run II of the Fermilab Tevatron or at the CERN Large Hadron Collider (LHC). After this discovery stage it will be important to analyze the properties of these sparticles and to check whether they have the correct quantum numbers to be partners of the SM particles.

While hadron colliders have the advantage of large available center-of-mass energy, they also have serious disadvantages: First, they produce enormous backgrounds from SM processes making it difficult to distinguish the signal from the background. Second, the remnants of the initial hadrons make it impossible to reconstruct the full final state. Third, the energies of the partons initiating the hard scattering are unknown so that an energy (mass) scan becomes impossible.

In e^+e^- annihilation, the full center-of-mass energy participates in the hard scattering and is precisely known, and the final state consists of a small number of high-energetic particles. The precision studies following upon the SUSY discovery stage are therefore the natural domain of high-energy lepton colliders. Important information on the SUSY parameters can be gained from the SUSY mass spectrum: It will be important to know whether all sfermions, squarks and sleptons, or those of the same generation, have identical mass parameters and/or gauge couplings, how large the differences and ratios among them are, or how much the left- and right-handed squarks or sleptons are mixed [1].

Currently several linear e^+e^- colliders in the 500–3000 GeV center-of-mass energy range are under design in various international collaborations. From previous experience with existing lepton colliders such as the CERN e^+e^- collider LEP2 it is well known that photons will be ubiquitous at future lepton colliders due to bremsstrahlung and beamstrahlung effects. Furthermore, it has been proposed to backscatter laser photons from the lepton beams in order to build a collider with high-energetic and almost monochromatic photon beams [2]. Photon colliders have similar advantages as lepton colliders: In energy scans the initial photon energy is known, although only to $\pm 15\%$, and the final state can be completely reconstructed.

Sfermion production in photon collisions has been considered previously either with bremsstrahlung photons [3,4] or with laser photons, where the center-of-mass energy dependence for fixed sfermion mass was analyzed in [5,6] and the sfermion mass dependence for a fixed collider energy of 1 TeV in [7,8]. The production of bound squarkonium states was considered in [9] for bremsstrahlung photons and in [10] for photon colliders.

In this paper we present the first complete analysis of sfermion production in photon-photon collisions from bremsstrahlung, beamstrahlung, and laser backscattering, including resolved photon processes and polarization effects. We compare the total cross sections directly to those in e^+e^- annihilation and also present differential cross sections. A FORTRAN program to generate total or differential cross sections for any sfermion type in polarized or unpolarized photon-photon collisions or in e^+e^- annihilation is available from the authors upon request.

In Sec. II we review for completeness the unpolarized photon spectra coming from bremsstrahlung, beamstrahlung, and laser backscattering and update them using the latest linear collider design parameters. In Sec. III we present our analytical and numerical results for sfermion production in unpolarized photon-photon collisions and compare them to those in e^+e^- annihilation. Section IV contains a discussion of polarized photon spectra. In Sec. V we calculate analytically and numerically total and differential cross sections for sfermion production in polarized photon-photon collisions. Our conclusions are given in Sec. VI.

II. UNPOLARIZED PHOTON SPECTRA

High energy electron-positron colliders are abundant sources of photons due to the presence of three photon pro-

duction mechanisms: bremsstrahlung, beamstrahlung, and laser backscattering. While the first two radiation processes occur at any circular or linear e^+e^- collider, albeit at different levels, laser backscattering requires additional laser beams and focusing mirrors, which may also interfere with the design of the detectors. These modifications still pose technical difficulties, and they will also increase the cost of such a ''photon collider.''

Bremsstrahlung can be conveniently described through an approximation of the complete two-photon process $e^+e^- \to e^+e^-X$. The outgoing photon spectrum is given by the Weizsäcker-Williams formula [11]

$$f_{\gamma/e}^{\rm brems}(x)=\frac{\alpha}{2\pi}\left[\frac{1+(1-x)^2}{x}\ln\frac{Q_{\rm max}^2(1-x)}{m_e^2x^2}+2m_e^2x\left(\frac{1}{Q_{\rm max}^2}-\frac{1-x}{m_e^2x^2}\right)\right]. \quad (1)$$

It has been integrated over the photon virtuality up to an upper bound $Q_{\rm max}^2=4E_e^2(1-x)$ for untagged outgoing electrons, which depends on the electron (positron) beam energy $E_e=\sqrt{S}/2$. This leads to a logarithmic dependence of the spectrum on S, the squared center-of-mass energy of the collider. $\alpha=e^2/(4\pi)=\sqrt{2}G_Fm_W^2s_W^2/\pi$ is the electromagnetic coupling constant in the G_F scheme, where G_F is the Fermi coupling constant, $s_W=\sqrt{1-(m_W/m_Z)^2}$ is the sine of the electroweak mixing angle, and $m_Z=91.188$ GeV and $m_W=80.419$ GeV are the masses of the electroweak gauge bosons. m_e is the electron mass, and x is the fractional energy of the photon in the electron.

At existing electron-positron or electron-proton colliders such as LEP2 and the DESY ep collider HERA, bremsstrahlung is the only relevant source of photons. Future circular electron-positron colliders above $\sqrt{S}=500$ GeV would suffer from very high synchrotron radiation. They must therefore have a linear design with large luminosities and dense particle bunches. Inside the opposite bunch, electrons and positrons experience transverse acceleration and radiate beamstrahlung. The corresponding spectrum [12]

$$f_{\gamma/e}^{\rm beam}(x)=\frac{5}{4\sqrt{3}\Upsilon}\int_u^\infty {\rm d}v\,{\rm Ai}(v)\left[\left(\frac{2v}{u}-1\right)\frac{1+(1-x)^2}{2(1-x)}+\frac{x^2}{2(1-x)}\right], \quad (2)$$

where the Airy function ${\rm Ai}(v)$ falls off exponentially at large v and $u=\{5x/[4\sqrt{3}\Upsilon(1-x)]\}^{2/3}$, is controlled by the beamstrahlung parameter

$$\Upsilon=\frac{5r_e^2E_eN}{6\alpha\sigma_z(\sigma_x+\sigma_y)m_e}. \quad (3)$$

This parameter is proportional to the effective electromagnetic field of the bunches and depends on the classical electron radius $r_e=\alpha/m_e=2.818\times10^{-15}$ m, on the rms sizes of the Gaussian beam σ_x, σ_y, σ_z, and on the total number of particles in a bunch N. Current design parameters for future linear colliders are listed in Table I [13].

TABLE I. Current design parameters for possible future linear colliders.

Collider	TESLA	JLC	NLC	CLIC
Last update	8/98	9/99	12/98	9/99
Center-of-mass energy (GeV)	500	500	500	500
Particles per bunch (10^{10})	2	1.11	0.95	0.4
σ_x (nm)	553	318	330	202
σ_y (nm)	5	4.3	4.9	2.5
σ_z (μm)	400	200	120	30
Υ	0.038	0.074	0.101	0.280
Center-of-mass energy (GeV)	800	1000	1000	1000
Particles per bunch (10^{10})	1.41	1.39	0.95	0.4
σ_x (nm)	391	318	234	115
σ_y (nm)	2	3.14	3.9	1.75
σ_z (μm)	300	200	120	30
Υ	0.082	0.186	0.285	0.979

For not too large $\Upsilon\leqslant5$ the spectrum for multiple photon emission can be written in the approximate form [14]

$$f_{\gamma/e}^{\rm beam}(x)=\frac{1}{\Gamma(\frac{1}{3})}\left(\frac{2}{3\Upsilon}\right)^{1/3}x^{-2/3}(1-x)^{-1/3}\times\exp\left[-\frac{2x}{3\Upsilon(1-x)}\right]\times\left\{\frac{1-\sqrt{\Upsilon/24}}{g(x)}\left[1-\frac{1}{g(x)N_\gamma}(1-e^{-g(x)N_\gamma})\right]+\sqrt{\frac{\Upsilon}{24}}\left[1-\frac{1}{N_\gamma}(1-e^{-N_\gamma})\right]\right\}, \quad (4)$$

where

$$g(x)=1-\frac{1}{2}[(1+x)\sqrt{1+\Upsilon^{2/3}}+1-x](1-x)^{2/3} \quad (5)$$

and the average number of photons radiated per electron throughout the collision is

$$N_\gamma=\frac{5\alpha^2\sigma_zm_e}{2r_eE_e}\frac{\Upsilon}{\sqrt{1+\Upsilon^{2/3}}}. \quad (6)$$

Since $\Upsilon\propto\sqrt{S}$, the exponential suppression of beamstrahlung decreases with rising $\sqrt{S}$ and from up to down in Table I. Beamstrahlung is most important for the CERN Compact Linear Collider (CLIC) design and less important for the Next Linear Collider (NLC), Japan Linear Collider (JLC), or DESY TeV Energy Superconducting Linear Accelerator (TESLA) designs.

The photon spectra for the $\sqrt{S}=1$ TeV e^+e^- colliders listed in Table I are shown in Fig. 1, where we have used the beamstrahlung spectrum of Eq. (4). It is obvious that the

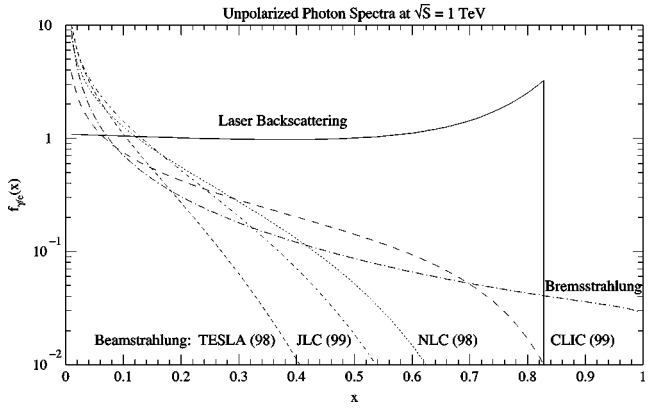

FIG. 1. Photon spectra for $\sqrt{S}=1$ TeV e^+e^- colliders. For TESLA, the 1998 beam size parameters of the $\sqrt{S}=0.8$ TeV design have been used.

bremsstrahlung and beamstrahlung mechanisms produce mostly soft photons. However, it is interesting to note that beamstrahlung at a 3 TeV CLIC collider [15] produces already 3 times more high-energetic photons (at $x=0.8$) than bremsstrahlung alone.

The situation is much better if laser photons are backscattered off the incident lepton beams. The laser backscattering spectrum [2]

$$f_{\gamma/e}^{\text{laser}}(x)=\frac{1}{N_c}\left[1-x+\frac{1}{1-x}-\frac{4x}{X(1-x)}+\frac{4x^2}{X^2(1-x)^2}\right], \tag{7}$$

where

$$N_c=\left[1-\frac{4}{X}-\frac{8}{X^2}\right]\ln(1+X)+\frac{1}{2}+\frac{8}{X}-\frac{1}{2(1+X)^2} \tag{8}$$

is related to the total Compton cross section, depends on the center-of-mass energy of the electron-laser photon collision $X=4E_eE_\gamma/m_e^2$. The optimal value of X is determined by the threshold for the process $\gamma\gamma\to e^+e^-$ and is $X=2+\sqrt{8}\simeq 4.83$ [16]. If this value is kept fixed, the laser backscattering spectrum becomes independent of $\sqrt{S}$. A large fraction of the photons is then produced close to the kinematic limit $x<x_{\max}=X/(1+X)\simeq 0.828$, so that one obtains an almost monochromatic ''photon collider.''

III. UNPOLARIZED CROSS SECTIONS

The inclusive cross section for photoproduction of sfermions in electron-positron collisions,

$$\sigma_{e^+e^-}^B(S)=\int \mathrm{d}x_1 f_{i/e}(x_1)\mathrm{d}x_2 f_{j/e}(x_2)\mathrm{d}t_{\tilde f}\mathrm{d}u_{\tilde f}\frac{\mathrm{d}^2\sigma_{ij}^B(s)}{\mathrm{d}t_{\tilde f}\mathrm{d}u_{\tilde f}}, \tag{9}$$

can be obtained by convolving the hard photonic cross section

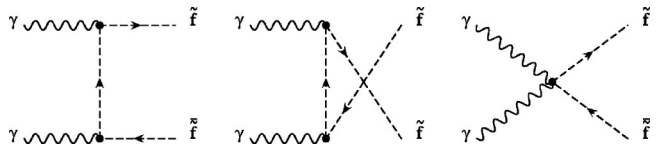

FIG. 2. Leading order Feynman diagrams for direct sfermion production in photon-photon collisions.

$$\frac{\mathrm{d}^2\sigma_{ij}^B(s)}{\mathrm{d}t_{\tilde f}\mathrm{d}u_{\tilde f}}=\frac{\pi(4\pi)^{-2+\varepsilon}}{s^2\Gamma(1-\varepsilon)}\left[\frac{t_{\tilde f}u_{\tilde f}-m_{\tilde f}^2 s}{\mu^2 s}\right]^{-\varepsilon}\Theta(t_{\tilde f}u_{\tilde f}-m_{\tilde f}^2 s)\times\Theta(s-4m_{\tilde f}^2)\,\delta(s+t_{\tilde f}+u_{\tilde f})\overline{|\mathcal{M}_{ij}^B|^2} \tag{10}$$

with the photon energy spectra $f_{\gamma/e}(x)$ discussed in the previous section. We denote the momenta of the massless incoming photons by $k_{1,2}$ and those of the outgoing sfermions with mass $m_{\tilde f}$ by $p_{1,2}$. Here $s=(k_1+k_2)^2=x_1x_2S$, $t_{\tilde f}=(k_2-p_2)^2-m_{\tilde f}^2$, and $u_{\tilde f}=(k_1-p_2)^2-m_{\tilde f}^2$ are the Mandelstam variables of the hard photon-photon scattering process. $\overline{|\mathcal{M}_{ij}^B|^2}$ is the partonic matrix element squared, summed (averaged) over final (initial) state spins and calculated in $d=4-2\varepsilon$ dimensions. μ is an arbitrary scale parameter. In addition to the direct contributions with $i,j=\gamma$, one or two of the photons can also resolve into a hadronic structure before they interact. For these single- and double-resolved contributions, the photon spectra $f_{\gamma/e}(x)$ have to be convolved with the parton density functions $f_{i,j/\gamma}(y)$ of quarks or gluons in the photons:

$$f_{i,j/e}(x)=\int_x^1\frac{\mathrm{d}y}{y}f_{\gamma/e}\left(\frac{x}{y}\right)f_{i,j/\gamma}(y). \tag{11}$$

The parton densities in the photon cannot be calculated in perturbation theory but have to be fitted to experimental data, e.g., on the photon structure function $F_2^\gamma(x)$ or on jet photoproduction.

In contrast, the partonic matrix elements can be calculated in perturbation theory. Direct sfermion production in leading order proceeds through the three diagrams shown in Fig. 2. The corresponding matrix element is given by

$$\overline{|\mathcal{M}_{\gamma\gamma}^B|^2}=\frac{4e^4e_{\tilde f}^4N_C[(1-\varepsilon)t_{\tilde f}^2u_{\tilde f}^2-2m_{\tilde f}^2t_{\tilde f}u_{\tilde f}s+2m_{\tilde f}^4s^2]}{(1-\varepsilon)^2t_{\tilde f}^2u_{\tilde f}^2}. \tag{12}$$

Here, summing over left- and right-handed squarks and sleptons has led to an additional factor of 2, but we do not sum over different sfermion generations. The color factor $N_C=3$ for squarks and $N_C=1$ for sleptons. Because of the large mass of the top quark, the supersymmetric partners of the left- and right-handed top, $\tilde t_{L,R}$, can mix to $\tilde t_{1,2}$ as can those of the bottom quark. It is important to note that the direct photon-photon cross section is proportional to the fourth power of the sfermion charge $ee_{\tilde f}$ ($e_{\tilde u}=2/3$, $e_{\tilde d}=-1/3$, $e_{\tilde l}=-1$). The cross section is independent of the details of the SUSY breaking mechanism, since it depends only on the physical sfermion masses $m_{\tilde f}$.

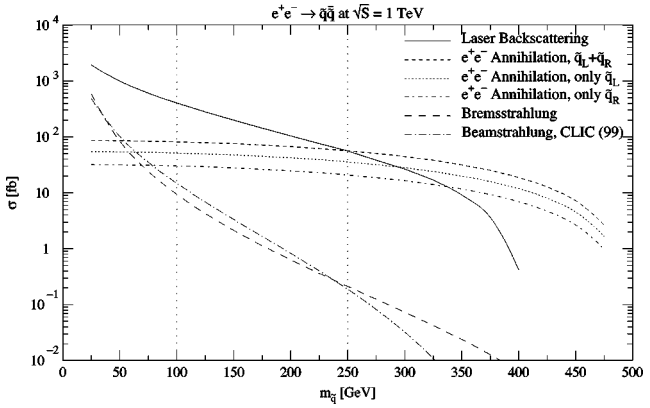

FIG. 3. Total cross sections for up-type squark ($\tilde{q}_L+\tilde{q}_R$) production in photon-photon scattering and in e^+e^- annihilation at a 1 TeV collider as a function of the squark mass.

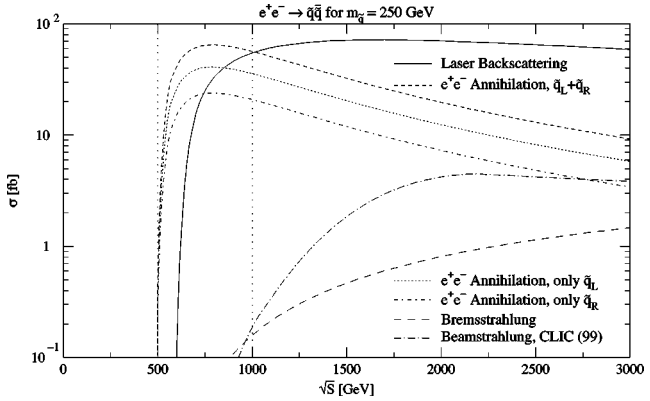

FIG. 4. Total cross sections for the production of up-type squarks ($\tilde{q}_L+\tilde{q}_R$) of mass 250 GeV in photon-photon scattering and in e^+e^- annihilation as a function of the center-of-mass energy.

This is different in electron-positron annihilation, where the squared matrix element [22]

$$\overline{|\mathcal{M}^B_{e^+e^-}|^2}=\frac{2\delta_{ij}e^4e_{\tilde{f}}^2N_C(t_{\tilde{f}}u_{\tilde{f}}-m_{\tilde{f}}^2s)}{s^2}+\frac{a_{ij}^2e^4N_C(1-4s_W^2+8s_W^4)(t_{\tilde{f}}u_{\tilde{f}}-m_{\tilde{f}}^2s)}{64s_W^4c_W^4[s^2+m_Z^4+m_Z^2(-2s+\Gamma_Z^2)]}+\frac{a_{ij}\delta_{ij}e^4e_{\tilde{f}}N_C(s-m_Z^2)(1-4s_W^2)(t_{\tilde{f}}u_{\tilde{f}}-m_{\tilde{f}}^2s)}{4s_W^2c_W^2s[s^2+m_Z^4+m_Z^2(-2s+\Gamma_Z^2)]} \tag{13}$$

depends on the details of the SUSY breaking mechanism through the sfermion mixing angle $\theta_{\tilde{f}}$ in the $Z^0\tilde{f}_i\bar{\tilde{f}}_j$ coupling $e/(4s_Wc_W)a_{ij}$ with

$$a_{ij}=\begin{pmatrix} 4(I_f^{3L}\cos^2\theta_{\tilde{f}}-e_{\tilde{f}}s_W^2) & -2I_f^{3L}\sin 2\theta_{\tilde{f}} \\ -2I_f^{3L}\sin 2\theta_{\tilde{f}} & 4(I_f^{3L}\sin^2\theta_{\tilde{f}}-e_{\tilde{f}}s_W^2)\end{pmatrix}, \tag{14}$$

and it is possible to produce off-diagonal sfermion mass eigenstates $\tilde{f}_i\bar{\tilde{f}}_j$. In this paper we restrict ourselves to the case of no squark mixing. $s_W(c_W)$ is the sine (cosine) of the electroweak mixing angle θ_W and $I_f^{3L}=1/2(-1/2)$ for up-type (down-type) fermions f. The first term in Eq. (13) corresponds to the exchange of a photon in the s channel, the second one to the exchange of a Z^0 boson, and the third one to the interference between the two. The cross section for the production of sfermions in electron-positron annihilation,

$$\sigma^B_{e^+e^-}(S)=\int \mathrm{d}t_{\tilde{f}}\mathrm{d}u_{\tilde{f}}\frac{\mathrm{d}^2\sigma^B_{e^+e^-}(S)}{\mathrm{d}t_{\tilde{f}}\mathrm{d}u_{\tilde{f}}}, \tag{15}$$

does of course not depend on the photon spectra or parton densities.

In Fig. 3 we show the total cross section for up-type squark production in photon-photon scattering and in e^+e^- annihilation at $\sqrt{S}=1$ TeV as a function of the squark mass. Only the annihilation cross section differs for left- and right-handed squarks. It extends out to $m_{\tilde{q}}\leqslant\sqrt{S}/2$. With laser backscattering, the mass range is reduced to $m_{\tilde{q}}\leqslant 0.8\sqrt{S}/2$. However, the photoproduction cross section exceeds the annihilation cross section for $m_{\tilde{q}}\leqslant 250$ GeV by up to an order of magnitude, and even above 250 GeV it is of comparable size. While up-type squarks below 250 GeV are already excluded by current Tevatron data, a light top squark and sleptons with $m_{\tilde{t}_1,\tilde{l}}>100$ GeV are still allowed [17–19]. These sparticles can therefore better be studied at a photon collider. Note that the photon cross section for light left- (right-) handed sfermions has to be divided by 2 and compared to the left- (right-) handed annihilation cross section. Slepton cross sections are larger than up-type squark cross sections by a factor $1/(3e_u^4)=27/16$, while down-squark cross sections are smaller by a factor $(e_{\tilde{d}}/e_{\tilde{u}})^4=1/16$. In addition, selectron production in e^+e^- annihilation has an additional contribution from the t-channel exchange of a neutralino. In Fig. 3 we also show the cross sections for photons produced with bremsstrahlung and beamstrahlung without additional laser facilities. We find that the bremsstrahlung cross section is of similar size as e^+e^- annihilation only for very light squarks, $m_{\tilde{q}}\leqslant 100$ GeV, which are already excluded experimentally. The bremsstrahlung cross section is always lower than the laser cross section by one to three orders of magnitude. Beamstrahlung, which is most important for the CLIC (99) design, behaves similarly to bremsstrahlung and enhances the bremsstrahlung cross section by a factor of 2.[1]

In Fig. 4 we show the cross sections for the production of up-type squarks of mass 250 GeV as a function of the center-of-mass energy of the collider. The annihilation cross section has a maximum at $\sqrt{S}\sim 3m_{\tilde{q}}$. At the kinematic limit of the collider, sfermions can only be produced through the annihilation process, but the laser backscattering cross section also shows a very steep threshold behavior. At higher energies,

[1]Our results agree with [4] for e^+e^- annihilation, but differ for the bremsstrahlung cross sections by approximately a factor of 3.

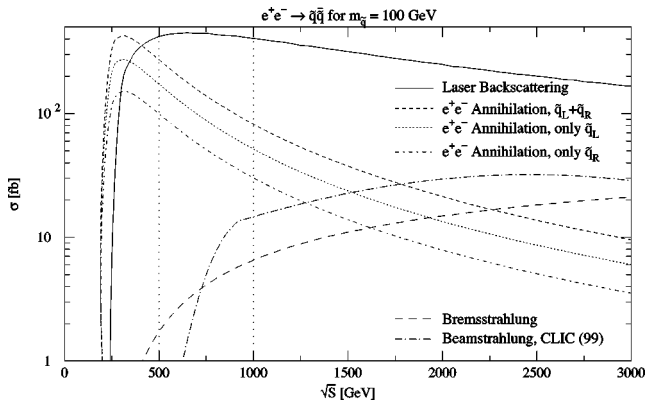

FIG. 5. Total cross sections for the production of up-type $(\tilde{q}_L+\tilde{q}_R)$ squarks of mass 100 GeV in photon-photon scattering and in e^+e^- annihilation as a function of the center-of-mass energy.

the laser backscattering cross section stays constant, while the annihilation cross section falls off like $1/S$. At 1 TeV or higher center-of-mass energy a photon collider is therefore favorable. At a very large energy CLIC collider even the bremsstrahlung and beamstrahlung cross sections become comparable to the annihilation cross section. For the beamstrahlung cross section it is necessary to interpolate between $\sqrt{S}=500$, 1000, and 3000 GeV, since the CLIC (99) design parameters are only known for these fixed center-of-mass energies.

For a light top squark and sleptons of mass $m_{\tilde{t}_1,\tilde{l}} \simeq 100$ GeV a photon collider is already favorable at the threshold of the sfermion pair production process in photon-photon collisions $[2\times 100\ \text{GeV}/0.8=250\ \text{GeV}]$, and the cross section falls off very slowly at large energies. This can be seen from Fig. 5 where we show total cross sections for the production of up-type squarks of mass 100 GeV. Even the bremsstrahlung and beamstrahlung cross sections for these light sparticles become interesting around $\sqrt{S}=1$ TeV.

As mentioned at the beginning of this section, photons can produce sfermions not only by direct coupling, but also after resolving into a hadronic structure. The direct, single, and double-resolved hard scattering matrix elements are formally of $\mathcal{O}(\alpha^2)$, $\mathcal{O}(\alpha\alpha_s)$, and $\mathcal{O}(\alpha_s^2)$, where α and α_s are the electromagnetic and strong coupling constants. However, the resolved processes have to be convolved with parton densities in the photon, which are of $\mathcal{O}(\alpha/\alpha_s)$ at asymptotically large factorization scales $\mu=m_{\tilde{q}}$. Therefore all three categories end up being of the same order $\mathcal{O}(\alpha^2)$ in the perturbative expansion. In resolved processes, only part of the initial photon energy participates in the hard scattering. Therefore one expects them to be important only at low masses, where not the full center-of-mass energy is needed.

If one of the two photons still couples directly, we obtain the contributions shown in Fig. 6. The matrix element squared for the process $\gamma g \to \tilde{q}\bar{\tilde{q}}$,

$$\overline{|\mathcal{M}^B_{\gamma g}|^2}=\frac{e^2e_{\tilde{q}}^2g_s^2C_F[(1-\varepsilon)t_{\tilde{q}}^2u_{\tilde{q}}^2-2m_{\tilde{q}}^2t_{\tilde{q}}u_{\tilde{q}}s+2m_{\tilde{q}}^4s^2]}{2(1-\varepsilon)^2N_CC_Ft_{\tilde{q}}^2u_{\tilde{q}}^2}, \tag{16}$$

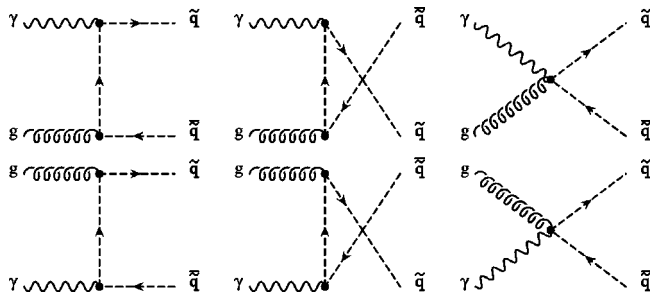

FIG. 6. Leading order Feynman diagrams for single-resolved sfermion production in photon-photon collisions. Initial state quarks contribute only at next-to-leading order.

can be obtained from the direct contribution by the replacements $e^2e_{\tilde{f}}^2 \to g_s^2$ and $N_C \to C_F/(2N_CC_F)$, where $g_s^2/(4\pi)=\alpha_s(\mu)$ is the strong coupling constant and $C_F=(N_C^2-1)/(2N_C)$ is the color factor of SU(3). The matrix element squared for the process $g\gamma \to \tilde{q}\bar{\tilde{q}}$ is identical. Obviously resolved contributions arise only for squarks, since sleptons do not couple strongly. The single-resolved matrix elements have to be convolved with the gluon density in the photon, which constitutes a higher order $\mathcal{O}(\alpha/\alpha_s\times\alpha_s)$ contribution to the photon structure and is not well constrained from deep-inelastic $e\gamma$ scattering. The gluon density is expected to be small at large $x=2m_{\tilde{q}}/\sqrt{s}$.

If both photons resolve into a hadronic structure, we obtain the contributions in Fig. 7. The matrix elements squared for the processes $q_i\bar{q}_j \to \tilde{q}\bar{\tilde{q}}$ and $gg \to \tilde{q}\bar{\tilde{q}}$ are

$$\begin{aligned}\overline{|\mathcal{M}^B_{q_i\bar{q}_j}|^2}=\frac{\delta_{ij}}{4N_C^2}\Bigg[&8g_s^4N_CC_F\frac{t_{\tilde{q}}u_{\tilde{q}}-m_{\tilde{q}}^2s}{s^2}\\&+4\hat{g}_s^4N_CC_F\frac{t_{\tilde{q}}u_{\tilde{q}}-(m_{\tilde{q}}^2-m_{\tilde{g}}^2)s}{(t-m_{\tilde{g}}^2)^2}\\&-8g_s^2\hat{g}_s^2C_F\frac{t_{\tilde{q}}u_{\tilde{q}}-m_{\tilde{q}}^2s}{s(t-m_{\tilde{g}}^2)}\Bigg]\\&+\frac{1-\delta_{ij}}{4N_C^2}\left[4\hat{g}_s^4N_CC_F\frac{t_{\tilde{q}}u_{\tilde{q}}-(m_{\tilde{q}}^2-m_{\tilde{g}}^2)s}{(t-m_{\tilde{g}}^2)^2}\right],\end{aligned} \tag{17}$$

$$\begin{aligned}\overline{|\mathcal{M}^B_{gg}|^2}=&\frac{4g_s^4}{16(1-\varepsilon)^2N_C^2C_F^2}\left[C_O\left(1-2\frac{t_{\tilde{q}}u_{\tilde{q}}}{s^2}\right)-C_K\right]\\&\times\left[1-\varepsilon-2\frac{sm_{\tilde{q}}^2}{t_{\tilde{q}}u_{\tilde{q}}}\left(1-\frac{sm_{\tilde{q}}^2}{t_{\tilde{q}}u_{\tilde{q}}}\right)\right],\end{aligned} \tag{18}$$

where $C_O=N_C(N_C^2-1)$, $C_K=(N_C^2-1)/N_C$, and $\hat{g}_s$ is the quark-squark-gluino Yukawa coupling, which is equal to the quark-quark-gluon gauge coupling g_s in leading order of SUSY-QCD. The t-channel contribution in $q_i\bar{q}_j \to \tilde{q}\bar{\tilde{q}}$ depends on the gluino mass $m_{\tilde{g}}$ and does not contribute for $\tilde{t}$

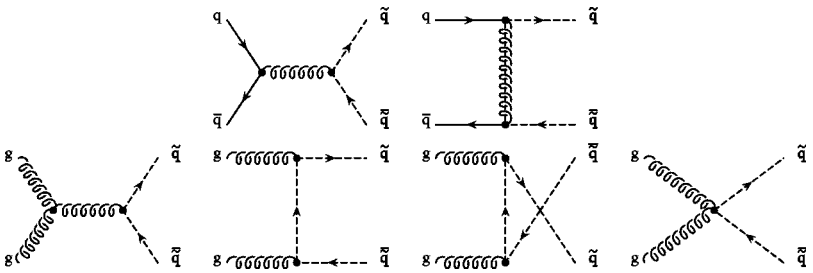

FIG. 7. Leading order Feynman diagrams for double-resolved sfermion production in photon-photon collisions.

production due to the negligible top quark density in the photon. Furthermore, the gluino-exchange t-channel term $\propto 1-\delta_{ij}$ is the only term through which off-diagonal squarks can be produced. Note that this is impossible in e^+e^- annihilation. The quark-initiated matrix elements have to be convolved with the leading order $\mathcal{O}(\alpha/\alpha_s)$ quark densities in the photon. These are fairly well constrained from deep-inelastic $e\gamma$ scattering and peak at $x\simeq 1$.

If we include all direct, single-resolved, and double-resolved contributions to up-type squark production in photon-photon scattering, we obtain the results shown in Fig. 8.

Here we have used the Glück-Reya-Vogt (GRV) [leading order (LO)] parton densities in the photon with a leading order value of $\alpha_s^{n_f=5}(\mu=m_{\tilde{q}})$ and $\Lambda^{(4)}=200$ MeV [20]. Resolved processes (mostly photon-gluon fusion) contribute substantially only at small squark masses (below 100 GeV), which are experimentally excluded. While the $q\bar{q}$ t channel varies by an order of magnitude with the gluino mass, this dependence does not show up in the total cross section. We have chosen gluino masses between the current experimental limit of 200 GeV [17] and 1 TeV, where weak-scale supersymmetry starts to become unnatural. The total cross section is clearly dominated by the direct channel and has very little dependence on resolved contributions or assumptions on the photon structure.

IV. POLARIZED PHOTON SPECTRA

Future lepton colliders are very likely to have a high degree of longitudinal polarization $|\lambda_e|\leqslant 1/2$. Part of this polarization will be transferred to the produced photons. The polarization state of the photon is determined by the Stokes parameters ξ_i, $i=1,2,3$ [21], where $\sqrt{\xi_1^2+\xi_3^2}$ is the degree of linear polarization and

$$\xi_2=\Delta f_{\gamma/e}(x)/f_{\gamma/e}(x), \quad \Delta f_{\gamma/e}(x)=f^+_{\gamma/e}(x)-f^-_{\gamma/e}(x) \tag{19}$$

is the mean helicity. Since ξ_1 and ξ_3 generally depend on the azimuthal angle, we will be mainly concerned with the circular polarization parameter ξ_2.

The circularly polarized bremsstrahlung spectrum

$$\Delta f^{\rm brems}_{\gamma/e}(x)=\frac{2\lambda_e\alpha}{2\pi}\left[\frac{1-(1-x)^2}{x}\ln\frac{Q^2_{\rm max}(1-x)}{m_e^2x^2}+2m_e^2x^2\left(\frac{1}{Q^2_{\rm max}}-\frac{1-x}{m_e^2x^2}\right)\right] \tag{20}$$

has been derived in [11]. As in the unpolarized case a nonlogarithmic term is present which is, however, not singular for $x\to 0$.

The x dependence of the circularly polarized beamstrahlung spectrum,

$$\Delta f^{\rm beam}_{\gamma/e}(x)=\frac{5\lambda_e}{2\sqrt{3}\Upsilon}\int_u^\infty dv\,{\rm Ai}(v)\left[\left(\frac{2v}{u}-1\right)\frac{1-(1-x)^2}{2(1-x)}+\frac{x^2}{2(1-x)}\right], \tag{21}$$

is very similar, as can be seen in Fig. 9. At $x\simeq 1$ the photons

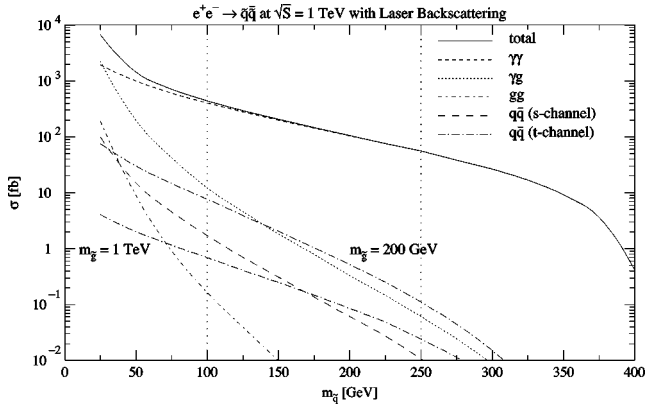

FIG. 8. Total, direct, and resolved cross sections for up-type squark ($\tilde{q}_L+\tilde{q}_R$) production at a 1 TeV photon collider as a function of the squark mass.

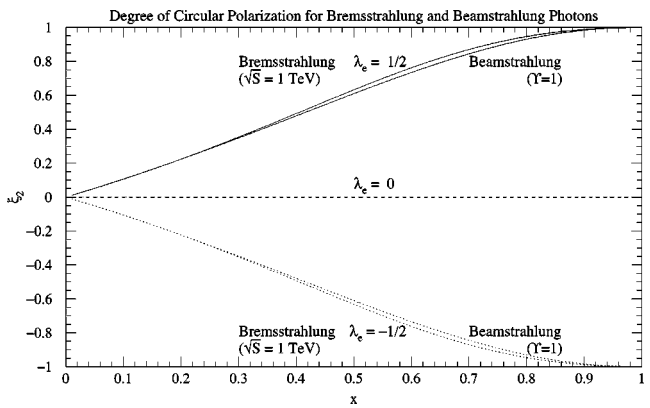

FIG. 9. Degree of circular polarization for bremsstrahlung and beamstrahlung photons.

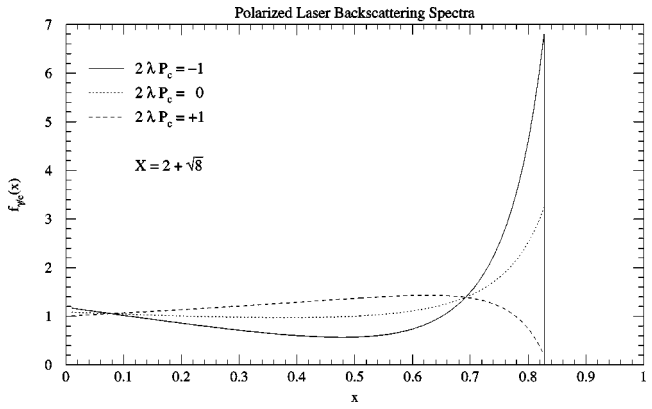

FIG. 10. Laser backscattering spectra for different combinations of electron and laser photon polarization $2\lambda_e P_c$.

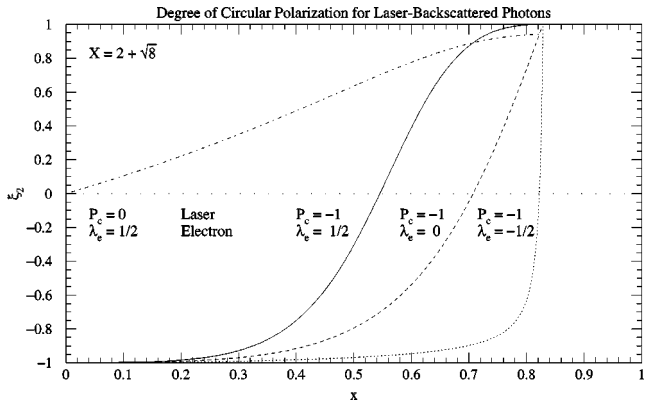

FIG. 11. Degree of circular polarization for laser-backscattered photons.

are completely polarized parallel to the incoming electron helicity, but at $x \simeq 0$, where most of the bremsstrahlung and beamstrahlung photons are produced, they are completely unpolarized. This can be understood from the fact that the electron polarization is lost in the Lorentz transformation from the Breit frame of the electron-photon vertex to the center-of-mass frame of the photon-target vertex. The dependence of ξ_2 on $\sqrt{S}$ and Υ is very weak. As $\Upsilon \to 100$, the beamstrahlung polarization coincides with the bremsstrahlung polarization. This discussion pertains strictly speaking only to single photon emission, but we expect a similar behavior also for multiple photon emission.

While the photon polarization at an e^+e^- collider is thus rather limited, a photon collider offers the additional possibility to control the helicity of the laser photons $|P_c| \leqslant 1$. This also affects the unpolarized photon spectrum [2]:

$$f^{\rm laser}_{\gamma/e}(x) = \frac{1}{N_c + 2\lambda_e P_c N_c'}\left[1 - x + \frac{1}{1-x} - \frac{4x}{X(1-x)} + \frac{4x^2}{X^2(1-x)^2} - 2\lambda_e P_c \frac{x(2-x)[x(X+2)-X]}{X(1-x)^2}\right], \tag{22}$$

where

$$N_c' = \left[\left(1 + \frac{2}{X}\right)\ln(1+X) - \frac{5}{2} + \frac{1}{1+X} - \frac{1}{2(1+X)^2}\right] \tag{23}$$

is related to the polarized total Compton cross section. As can be seen in Fig. 10, the monochromaticity of the outgoing photons can be improved considerably by choosing $2\lambda_e P_c = -1$.

Figure 11 shows the degree of circular polarization ξ_2 with

$$\Delta f^{\rm laser}_{\gamma/e}(x) = \frac{1}{N_c + 2\lambda_e P_c N_c'}\left\{2\lambda_e \frac{x}{1-x}\left[1 + (1-x)\times\left(1 - \frac{2x}{(1-x)X}\right)^2\right] + P_c\left(1 - \frac{2x}{(1-x)X}\right)\times\left(1 - x + \frac{1}{1-x}\right)\right\} \tag{24}$$

for laser-backscattered photons [2]. If only the electrons are polarized ($P_c = 0$), the result coincides again with that for bremsstrahlung and beamstrahlung. However, if $P_c = \pm 1$, then the backscattered photons have helicity $\xi_2 = -P_c$ at $x = x_{\rm max}$. Therefore the choice $2\lambda_e P_c = -1$ guarantees not only good monochromaticity, but also a high degree of circular polarization of the produced photons. By switching the signs of λ_e and P_c simultaneously, one can switch the helicity ξ_2 of the outgoing photons without changing the photon spectrum or spoiling its monochromaticity.

V. POLARIZED CROSS SECTIONS

The cross section for sfermion production in polarized photon-photon collisions can again be calculated from Eqs. (9) and (10). However, the unpolarized matrix element squared has to be replaced with

$$\overline{|\mathcal{M}^B_{\gamma\gamma}|}^2 = \frac{4e^4 e_{\tilde f}^4 N_C}{(1-\varepsilon)^2 t_{\tilde f}^2 u_{\tilde f}^2}\{(1-\varepsilon)t_{\tilde f}^2 u_{\tilde f}^2 \times[1 + \tilde\xi_1^{(1)}\tilde\xi_1^{(2)} - \tilde\xi_2^{(1)}\tilde\xi_2^{(2)} + \tilde\xi_3^{(1)}\tilde\xi_3^{(2)}] - 2m_{\tilde f}^2 t_{\tilde f} u_{\tilde f} s[\tilde\xi_1^{(1)}\tilde\xi_1^{(2)} - \tilde\xi_2^{(1)}\tilde\xi_2^{(2)} + (1+\tilde\xi_3^{(1)})(1+\tilde\xi_3^{(2)})] + 2m_{\tilde f}^4 s^2(1+\tilde\xi_3^{(1)}) \times(1+\tilde\xi_3^{(2)})\}, \tag{25}$$

which has been calculated using the covariant density matrix for polarized photons [21]:

$$\rho_{\mu\nu}^{(1,2)}=\varepsilon_\mu\varepsilon_\nu^*=\frac{1}{2}(e_\mu^x e_\nu^x+e_\mu^y e_\nu^y)\pm\frac{\xi_1^{(1,2)}}{2}(e_\mu^x e_\nu^y+e_\mu^y e_\nu^x)$$
$$\mp\frac{i\xi_2^{(1,2)}}{2}(e_\mu^x e_\nu^y-e_\mu^y e_\nu^x)+\frac{\xi_3^{(1,2)}}{2}(e_\mu^x e_\nu^x-e_\mu^y e_\nu^y). \tag{26}$$

The $\xi_i^{(1,2)}$, $i=1,2,3$, are the Stokes parameters discussed in the previous section. They describe the polarizations $\varepsilon_{\mu,\nu}^{(*)}$ of the photons with momenta $k_{1,2}=\sqrt{s}/2(1,0,0,\pm 1)$. Here e^x and e^y denote unit vectors in the x and y directions. The momenta of the outgoing sfermions are given by $p_{1,2}=(m_T\cosh y,\pm p_T\cos\phi,\pm p_T\sin\phi,\pm m_T\sinh y)$, and p_T, y, and ϕ are the transverse momentum, rapidity and azimuthal angle of the produced sfermions; $m_T=\sqrt{m_{\tilde f}^2+p_T^2}$ is the transverse sfermion mass. The azimuthal dependence of the cross section has been included in the rotated Stokes parameters:

$$\tilde\xi_1^{(1)}=\xi_1^{(1)}\cos(2\phi)-\xi_3^{(1)}\sin(2\phi), \tag{27}$$
$$\tilde\xi_2^{(1)}=\xi_2^{(1)},$$
$$\tilde\xi_3^{(1)}=\xi_1^{(1)}\sin(2\phi)+\xi_3^{(1)}\cos(2\phi),$$
$$\tilde\xi_1^{(2)}=\xi_1^{(2)}\cos(2\phi)+\xi_3^{(2)}\sin(2\phi),$$
$$\tilde\xi_2^{(2)}=\xi_2^{(2)},$$
$$\tilde\xi_3^{(2)}=-\xi_1^{(2)}\sin(2\phi)+\xi_3^{(2)}\cos(2\phi).$$

For sfermion production in polarized photon-photon collisions we consider only direct processes. Our analysis of the unpolarized cross section has clearly demonstrated that resolved processes are only important at very small, experimentally excluded, squark masses. Furthermore, almost nothing is known experimentally about polarized parton densities in the photon. Predictions for polarized resolved photoproduction would thus be very speculative.

Because of the azimuthal dependence, cross sections with linear photon polarization are difficult to disentangle and remain small if averaged over the azimuthal angle. Therefore we restrict ourselves to circularly polarized photons and set $\xi_1=\xi_3=0$. Since $\overline{|\mathcal{M}_{\gamma\gamma}^B|^2}$ depends then only the product $\tilde\xi_2^{(1)}\tilde\xi_2^{(2)}$, we expect identical cross sections for incoming photons with identical or opposite helicities.

In Fig. 12 we compare the e^+e^- annihilation cross section against the polarized photon-photon cross section for up-type squark production at a 1 TeV photon collider for different squark masses. The labels $++$, $--$, $+-$, and $-+$ denote the helicities P_c of the incoming laser photons. The helicities of the incoming leptons λ_e have always been chosen to ensure the condition for optimal monochromaticity, $2\lambda_e P_c=-1$. The backscattered photons are therefore highly polarized in the direction opposite to the laser photon (see Fig. 11). The unpolarized curve is the same as in Fig. 3, i.e., $\lambda_e=P_c=0$.

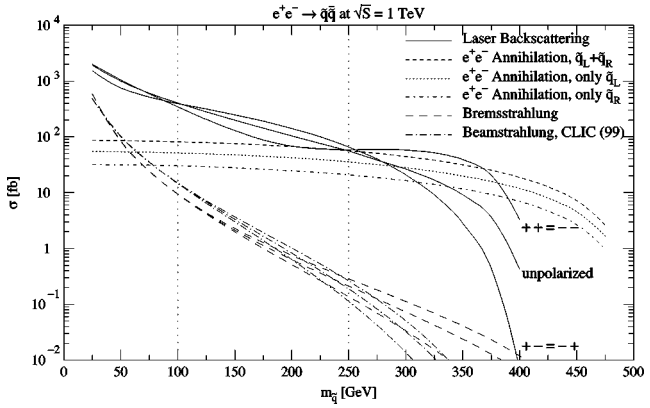

FIG. 12. Total cross sections for up-type squark ($\tilde q_L+\tilde q_R$) production in polarized photon-photon scattering and in e^+e^- annihilation at a 1 TeV collider as a function of the squark mass.

Figure 12 demonstrates that the unpolarized photon-photon cross section can be enhanced in the region $m_{\tilde f}\in[100;250]$ GeV by about 40% if one chooses opposite laser photon helicities ($+-$ or $-+$). For $m_{\tilde f}>250$ GeV the effect is even more dramatic: The cross section can be improved by almost an order of magnitude at large $m_{\tilde f}$ if one chooses identical laser photon helicities. The cross section at a polarized photon collider stays larger than the e^+e^- annihilation cross section almost up to the kinematic limit of the photon collider. It is interesting to note that one has to switch from opposite to identical helicities at $m_{\tilde f}\simeq 250$ GeV, where the unpolarized photon-photon cross section drops below the annihilation cross section. In Fig. 12 we also show polarization effects for sfermions produced via bremsstrahlung and beamstrahlung. The cross sections remain small and are only slightly enhanced by preferring identical over opposite lepton helicities.

In Fig. 13 we compare the same cross sections for a fixed up-type squark mass of 250 GeV as a function of the center-of-mass energy of the collider $\sqrt{S}$. The unpolarized photon cross section can again be enhanced by an appropriate choice of polarization. In particular, identical laser photon helicities

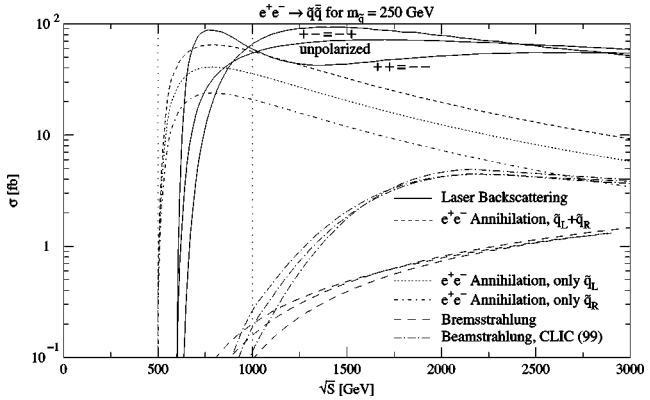

FIG. 13. Total cross sections for the production of up-type squarks ($\tilde q_L+\tilde q_R$) of mass 250 GeV in polarized photon-photon scattering and in e^+e^- annihilation as a function of the center-of-mass energy.

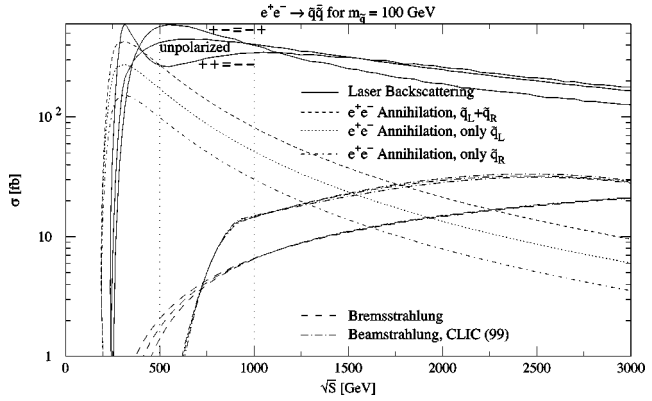

FIG. 14. Total cross sections for the production of up-type squarks ($\tilde{q}_L+\tilde{q}_R$) of mass 100 GeV in polarized photon-photon scattering and in e^+e^- annihilation as a function of the center-of-mass energy.

lead to a photon cross section which is larger than the annihilation cross section already at the threshold of the photon collider, i.e., below 1 TeV, while the cross section for opposite helicities is smaller by a factor $\beta^4=(1-4m_q^2/s)^2$. Polarization for bremsstrahlung and beamstrahlung is again of little interest. At large $\sqrt{S}$, where the cross sections become large, the radiated photons are completely unpolarized.

For up-type squarks of mass 100 GeV we show the center-of-mass energy dependence in Fig. 14. Again the cross section at threshold can be optimized by choosing identical photon helicities.

For experimental analyses it is also important to study differential cross sections, e.g., in the transverse momentum p_T or the rapidity y of the produced supersymmetric particles,

$$\frac{\mathrm{d}\sigma^B_{e^+e^-}(S)}{\mathrm{d}p_T\mathrm{d}y}=2p_TS\int \mathrm{d}x_1x_1f_{i/e}(x_1)\mathrm{d}x_2x_2f_{j/e}(x_2)\frac{\mathrm{d}^2\sigma^B_{ij}(s)}{\mathrm{d}t_{\tilde{f}}\mathrm{d}u_{\tilde{f}}}, \tag{28}$$

since cuts on p_T and y can help to eliminate backgrounds. For this reason we show in Fig. 15 differential p_T spectra for

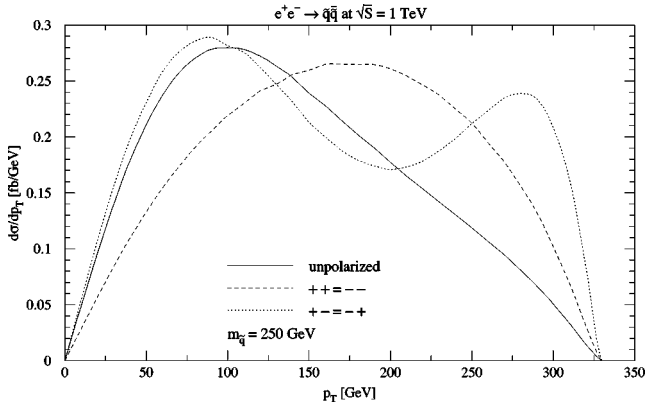

FIG. 15. Differential cross sections for the production of up-type squarks ($\tilde{q}_L+\tilde{q}_R$) of mass 250 GeV at a 1 TeV polarized photon collider as a function of the transverse momentum p_T.

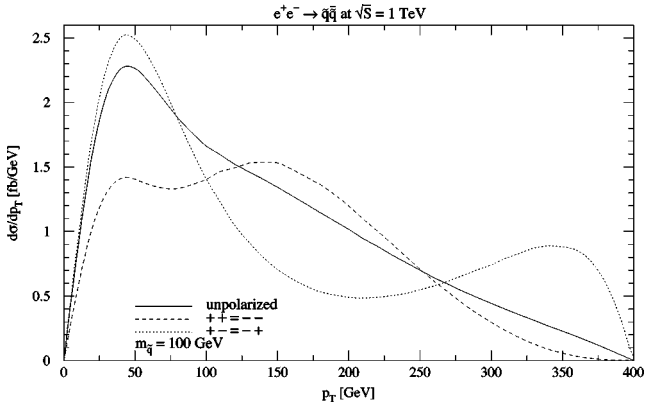

FIG. 16. Differential cross sections for the production of up-type squarks ($\tilde{q}_L+\tilde{q}_R$) of mass 100 GeV at a 1 TeV polarized photon collider as a function of the transverse momentum p_T.

up-type squarks of mass 250 GeV, produced at a 1 TeV photon collider. The spectra have been integrated over the rapidity y and extend out to the kinematic limit $p_T<0.828\sqrt{S}-2m_{\tilde{f}}=328$ GeV. While the unpolarized spectrum peaks at $p_T\simeq 100$ GeV, or roughly at $m_{\tilde{f}}/2$, the mean p_T of sfermions produced with backscattered laser photons of identical helicity is almost twice as big. If the laser photons have opposite helicity, one gets a distinct twin-peak behavior with a local minimum. This is due to the absence of the four-point interaction diagram in Fig. 2 which contributes only for identical helicities at intermediate p_T. These features should be very helpful in experimental analyses. Similar results for up-type squarks of mass 100 GeV are shown in Fig. 16.

Finally we show in Fig. 17 rapidity distributions for up-type squarks of mass 100 GeV produced at a 1 TeV photon collider. The rapidity spectra are symmetric at $y=0$ and extend out to $|y|<2$. This range should be covered by the detector at a photon collider to provide optimal analyzing conditions for sfermions of mass $m_{\tilde{f}}=100$ GeV. For $m_{\tilde{f}}=250$ GeV the rapidity spectrum is narrower and extends out to $|y|<1.1$ (see Fig. 18). The spectrum for laser photons with identical helicities is again very similar to the unpolar-

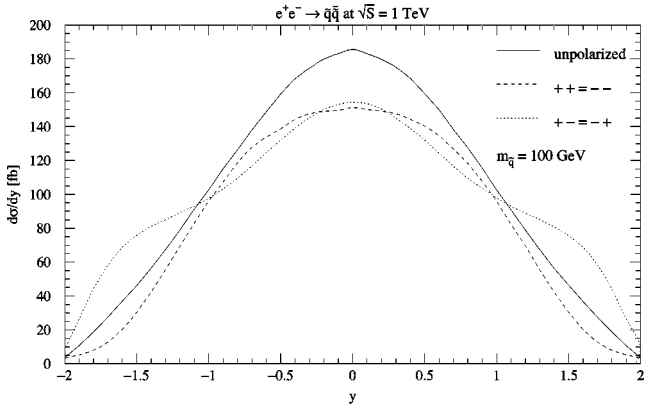

FIG. 17. Differential cross sections for the production of up-type squarks ($\tilde{q}_L+\tilde{q}_R$) of mass 100 GeV at a 1 TeV polarized photon collider as a function of the rapidity y.

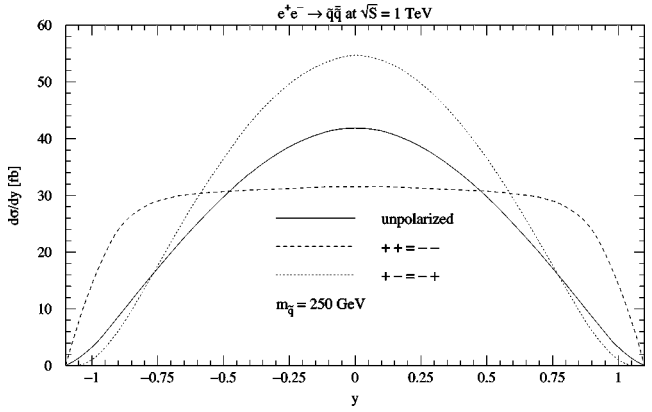

FIG. 18. Differential cross sections for the production of up-type squarks ($\tilde{q}_L + \tilde{q}_R$) of mass 250 GeV at a 1 TeV polarized photon collider as a function of the rapidity y.

ized spectrum. The spectrum for opposite helicities has interesting shoulders at $y = \pm 1.5$ in the case of $m_{\tilde{f}} = 100$ GeV. The dips at $y = \pm 1$ are again due to the absence of the four-point interaction diagram in Fig. 2 for opposite helicities.

VI. CONCLUSION

In this paper we have presented a detailed analysis of sfermion production in photon-photon collisions. We have reviewed the unpolarized and polarized photon spectra coming from bremsstrahlung, beamstrahlung, and laser backscattering and updated them using the latest linear collider design parameters. We have calculated for the first time total and differential cross sections for sfermion production in photon-photon collisions, including contributions from resolved photons and arbitrary photon polarization. Our numerical results have been compared directly to the competing e^+e^- annihilation cross section. We have chosen to present our results for the typical case of up-type squark production. The cross sections for down-type squarks and sleptons can easily be obtained by rescaling our results according to the sfermion charge and color factor.

Bremsstrahlung and beamstrahlung photons will be produced naturally at any linear e^+e^- collider. Our results show that the corresponding production cross sections are small, except at the very large center-of-mass energies envisaged in the CLIC design. The polarization of the initial photons remains small even if the initial lepton polarization is large. Therefore polarization effects in bremsstrahlung and beamstrahlung are of little interest.

A dedicated photon collider will require the construction of additional laser facilities at some extra cost. However, we have demonstrated that a photon collider may be advantageous for the analysis of sfermions for several reasons:

(i) In leading order of perturbation theory, photon-photon collisions are pure SUSY-QED processes, which depend only on the physical sfermion mass and not on the details of the SUSY breaking mechanism. Any model dependence can therefore be analyzed cleanly in the decay of the sfermions.

(ii) The photon cross section is very sensitive to the sfermion charge so that sleptons, up-type, and down-type squarks can be clearly distinguished.

(iii) A photon collider can produce almost monochromatic photons, i.e., photons which have about 83% of the electron beam energy, and they can be highly polarized. As a consequence we find that the production cross sections are larger than those in e^+e^- annihilation for a large range of sfermion masses. If the incoming laser photons and leptons are polarized and the photons have identical helicities, this is even true up to the kinematic limit of the photon collider. For lower sfermion masses or higher center-of-mass energies the cross section can be improved by about 40% by choosing opposite laser photon helicities.

Resolved photon processes are only important for squarks, since sleptons do not couple strongly. Furthermore, resolved photons contribute significantly only at very small squark masses, which are experimentally already excluded. While there is thus no enhancement of the production cross section, there is also no uncertainty due to the photon structure or the scale of the strong coupling constant.

Differential cross sections are important for experimental analyses to distinguish signal from background events. We find that the p_T spectrum for sfermion production in photon collisions peaks roughly at $m_{\tilde{f}}/2$ as expected. The rapidity spectrum for sfermions of mass $m_{\tilde{f}} = 100$ GeV at a 1 TeV photon collider extends out to ± 2. We conclude that this should be the minimum coverage a detector at a photon collider should have to ensure full analyzing power. The polarized p_T and y spectra have very distinct features which should be helpful in the experimental analysis.

ACKNOWLEDGMENTS

We thank D. V. Schroeder for mailing us a copy of his Ph.D. thesis and K. Hagiwara, B. A. Kniehl, G. Kramer, V. Telnov, and A. Tkabladze for valuable comments. This work has been supported by the Deutsche Forschungsgemeinschaft through Grant No. KL 1266/1-1 and Graduiertenkolleg *Zukünftige Entwicklungen in der Teilchenphysik* and by the European Commission through Grant No. ERBFMRX-CT98-0194.

[1] ECFA/DESY LC Physics Working Group Collaboration, E. Accomando *et al.*, Phys. Rep. **299**, 1 (1998).

[2] I. F. Ginzburg, G. L. Kotkin, V. G. Serbo, and V. I. Telnov, Nucl. Instrum. Methods Phys. Res. **205**, 47 (1983); I. F. Ginzburg, G. L. Kotkin, S. L. Panfil, V. G. Serbo, and V. I. Telnov, Nucl. Instrum. Methods Phys. Res. A **219**, 5 (1984).

[3] J. A. Grifols and J. Sola, Z. Phys. C **18**, 185 (1983).

[4] T. G. Rizzo, Phys. Rev. D **40**, 2803 (1989).

[5] F. Cuypers, G. J. van Oldenborgh, and R. Rückl, Nucl. Phys. **B409**, 144 (1993).

[6] C. Chang, L. Han, W. Ma, and Z. Yu, Nucl. Phys. **B515**, 15 (1998).
[7] V. Telnov, Nucl. Phys. (Proc. Suppl.) **82**, 359 (2000).
[8] D. Choudhury and A. Datta, hep-ph/0005082.
[9] I. I. Bigi and F. Gabbiani, Report No. UND-HEP-91-BIG05.
[10] D. S. Gorbunov and V. A. Ilyin, hep-ph/0004092.
[11] D. de Florian and S. Frixione, Phys. Lett. B **457**, 236 (1999).
[12] D. V. Schroeder, Report No. SLAC-0371.
[13] International Linear Collider Technical Review Committee, http://www.slac.stanford.edu/xorg/ilc-trc/ilc-trchome.html
[14] P. Chen, Phys. Rev. D **46**, 1186 (1992).
[15] Compact Linear Collider Study, http://cern.web.cern.ch/CERN/Divisions/PS/CLIC/Tables/TABLE1.html
[16] V. I. Telnov, Nucl. Instrum. Methods Phys. Res. A **294**, 72 (1990).
[17] Particle Data Group, D. E. Groom *et al.*, Eur. Phys. J. C **15**, 1 (2000).
[18] G. Cho and K. Hagiwara, Nucl. Phys. **B574**, 623 (2000).
[19] S. Alam, K. Hagiwara, S. Kanemura, R. Szalapski, and Y. Umeda, Phys. Rev. D **62**, 095011 (2000).
[20] M. Glück, E. Reya, and A. Vogt, Phys. Rev. D **45**, 3986 (1992).
[21] V. B. Berestetskii, E. M. Lifshitz, and L. P. Pitaevskii, *Relativistic Quantum Theory*, Course of Theoretical Physics Vol. 4 (Pergamon, New York, 1979).
[22] H. Eberl, A. Bartl, and W. Majerotto, Nucl. Phys. **B472**, 481 (1996).